Nucleation of Grain Boundary Phases

I. S. Winter,[1, *] R. E. Rudd,[1] T. Oppelstrup,[1] and T. Frolov[1, †]

[1]*Lawrence Livermore National Laboratory, Livermore, CA, 94550, USA*
(Dated: August 17, 2021)

We derive a theory that describes homogeneous nucleation of grain boundary (GB) phases. Our analysis takes account of the energy resulting from the GB phase junction, the line defect separating two different GB structures, which is necessarily a dislocation as well as an elastic line force due to the jump in GB stresses. The theory provides analytic forms for the elastic interactions and the core energy of the GB phase junction that, along with the change in GB energy, determine the nucleation barrier. We apply the resulting nucleation model to simulations of GB phase transformations in tungsten. Our theory explains why under certain conditions GBs cannot spontaneously change their structure even to a lower energy state.

The nucleation of a different phase of matter from a parent phase is one of the most basic phenomena studied within the physical sciences, and has tremendous impact on a range of technologies from the efficiency of steam engines [1] to engineering alloys [2]. Classical nucleation theory describes the energetics of homogeneous nucleation of a solid phase in a liquid phase using only two parameters: the difference in free energy between the two phases and the interfacial energy of the two phases [3]. The description of solid-solid phase transformations becomes more complicated due to the presence of elastic contributions to the nucleation energy [2], such as the elastic effects from an Eshelby inclusion [2, 4, 5] and dislocation strain fields[6].

Similarly to bulk materials, interfaces can also exhibit phase-like behavior [7–9]. For interfacial phases in fluid systems, the conditions of equilibrium and stability were first derived by Gibbs [10]. In solid systems, phase transformations and grain boundaries (GBs), interfaces formed by two misoriented crystals of the same material, has recently become a topic of increased interest due to the accumulating experimental and modeling evidence of first-order transitions at such interfaces [11–23]. GB phase transitions are important because they result in discontinuous changes in grain-boundary properties such as mobility, diffusivity, and cohesive strength. [16, 24–29]. These changes in turn can have a tremendous impact on macroscopic properties of materials such as creep and ductility by affecting a material's microstructure [30–36].

While GB phase transformations have now been seen in many different materials [9], the thermodynamics and kinetics of these transformations is not understood. In principle, a grain boundary with multiple possible structures of nearly the same energy should be able to sample its different states at finite temperature, making the GB structure an ensemble of different configurations [27, 37]. However, in experimental and modeling studies GBs behave more like conventional 3D phases: only one GB phase is observed at a time or, when a transformation occurs, the two GB phases are separated by a sharp 1D interface [11, 20, 23, 38, 39]. Moreover, GB phase transitions can be sluggish or delayed even when they

are not limited by solute diffusion [23, 40, 41]. Time-Temperature-Transformation (TTT) GB diagrams describing these kinetics have been proposed as a new strategy for GB engineering and optimization of materials properties [40, 41].

No nucleation theory currently exists explaining GB phase transformation behavior. A major gap is the poor understanding of the role of GB phase junctions, the 1D interfaces separating two different phases within a GB [42–46]. In this work, we use the classical nucleation theory (CNT) approach to describe GB phase transformations. The resulting theory recognizes that GB phase junctions are dislocations as well as elastic line forces and for the first time quantifies the contribution of their elastic interactions and core energy to the nucleation barrier.

Consider nucleation of a new GB phase α from a parent GB phase β, as shown in Fig. 1a. For simplicity, we assume that the nucleus is circular. Figure 1b shows the side view of the system in 1a which also includes the two misoriented crystals. GB phase junctions are dislocations as well as line forces, arising from the imbalance of the grain boundary stresses $\boldsymbol{\tau}^\beta$ and $\boldsymbol{\tau}^\alpha$: $\boldsymbol{f} = (\boldsymbol{\tau}^\alpha - \boldsymbol{\tau}^\beta) \cdot \hat{\boldsymbol{r}}$, where $\hat{\boldsymbol{r}}$ is the radial unit vector. The GB phase junction indicated on the figure as a contour $\boldsymbol{C}$ forms a closed circular loop, which is a dislocation loop of Burgers vector $\boldsymbol{b}$ [42] and line force $\boldsymbol{f}$. The energy of the nucleus is given by

$$E^{nuc}(R) = \pi R^2 \Delta\gamma^{\alpha\beta} + 2\pi R\bar{\Gamma}^{\alpha\beta} + E^{dd}(R) + E^{dp}(R) + E^{pp}(R), \tag{1}$$

Here the first two terms are the usual CNT contributions describing the driving force for the transformation due to the reduction in the GB free energy per unit area $\Delta\gamma^{\alpha\beta} = \gamma^\alpha - \gamma^\beta$ and the increase due to the perimeter energy, $\bar{\Gamma}^{\alpha\beta}$, the effective orientation-averaged core energy per unit length of the GB phase junction. The last three terms on the right hand side of Eq. (1) describe the elastic part of the GB phase junction energy. $E^{dd}(l)$ is the elastic self-energy of the dislocation loop, $E^{pp}(l)$ is the elastic energy of the line force loop, and $E^{dp}(l)$ is the interaction between the dislocation and line force loop. A detailed derivation is given in the Supplemental Materials. Each
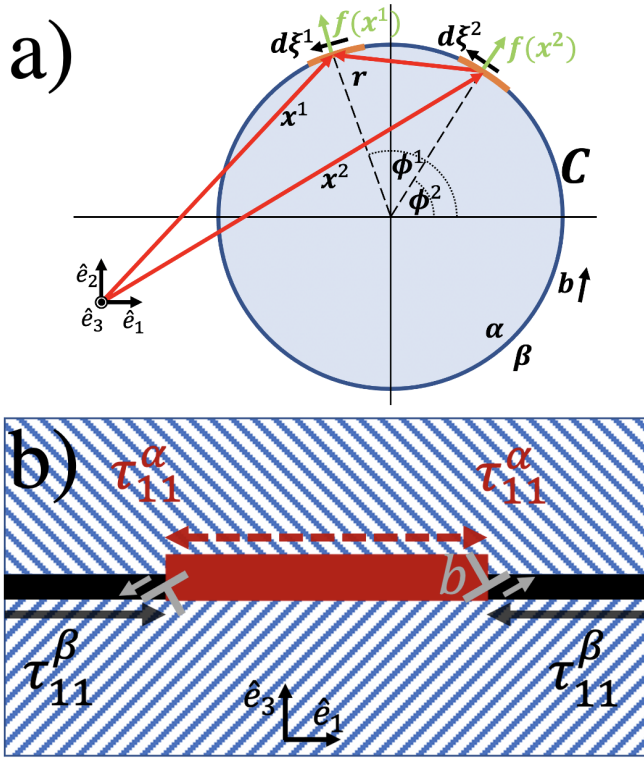
FIG. 1. Panel a depicts a top view of the GB plane showing a circular nucleus of GB phase α inside the parent GB phase β. The contour $\boldsymbol{C}$ represents the GB phase junction. Panel b shows a side view of a slice through the nucleus of GB phase β showing the misoriented bulk crystals and GB phases. Two GB phase junctions are indicated by dislocation symbols. The imbalance of GB stresses $\boldsymbol{\tau}^{\beta}$ and $\boldsymbol{\tau}^{\alpha}$ at GB phase junctions also produces line forces.

elastic term is given as:

$$
E^{dd}(R) = \frac{\mu R}{4(1-\nu)} \left[\left(2b_3^2 + (b^p)^2(2-\nu) \right) \ln\left(\frac{4R}{\rho}\right) \right.
$$
$$
\left. - 2\left(b_3^2 + (b^p)^2(2-\nu) \right) \right], \quad (2a)
$$

$$
E^{dp}(R) = -\frac{(f_1+f_2)b_3 R}{2(1-\nu)} \left[(1-2\nu)\ln(4R/\rho) - 3 + 4\nu \right], \quad (2b)
$$

$$
E^{pp}(R) = -\frac{R}{32\mu(1-\nu)} \left[\left(f^2(13-16\nu) \right. \right.
$$
$$
\left. \left. - 2f_1 f_2 \right) \ln(4R/\rho) - 4f^2(7-8\nu) \right]. \quad (2c)
$$

$(b^p)^2 = b_1^2 + b_2^2$. ρ is the core radius of the dislocation, and is b. b_3 is the $\hat{e}_3$ component of the Burgers vector; and $f^2 = f_1^2 + f_2^2$, $f_1 = (\tau_{11}^\alpha - \tau_{11}^\beta)$, and $f_2 = (\tau_{22}^\alpha - \tau_{22}^\beta)$.

Equations (1) and (2) describe the energetics of GB phase nucleation by predicting the energy of the nucleus

as a function of its size. Equation (1) incorporates the elastic energy due to the GB phase junctions and can be used to predict the size of the critical nucleus. In the 3D system considered here, the perimeter of the GB phase junction changes with the radius of the nucleus; as a result, the core energy $\bar{\Gamma}^{\alpha\beta}$ cannot be calculated directly from MD using this 3D model, but could be treated as a fitting perimeter. Before we proceed to the MD part of this study, we show that $\bar{\Gamma}^{\alpha\beta}$ can be calculated directly from molecular statics simulations of quasi-2D nucleation.

Consider a GB phase transformation in a quasi-2D system such as a thin film, schematically shown in Fig. 1b. Here the length of each GB phase junction is fixed and set by the film thickness, L. In this 2D case, the two GB phase junctions are dislocations and line forces, and the energy of the system per unit thickness as a function of nucleus width l is given by

$$
\frac{E^{2D}}{L} = \Delta\gamma^{\alpha\beta}l + \frac{E^{dd}}{L}(l) + \frac{E^{pp}}{L}(l) + \frac{E^{dp}}{L}(l) + 2\Gamma^{\alpha\beta}, \quad (3)
$$

This is the 2D analog of Eq. (1). In Eq. (3) the core energy $\Gamma^{\alpha\beta}$ is decoupled from the elastic energy terms. Since E^{2D} and $\Delta\gamma^{\alpha\beta}$ can be calculated directly from molecular statics calculations and the elastic energy terms can be evaluated using the elasticity theory, Eq. (3) and quasi-2d MD simulations of nucleation can be used to calculate $\Gamma^{\alpha\beta}$.

The three elastic energy terms are derived in the Supplemental Materials:

$$
\frac{E^{dd}}{L}(l) = \frac{\mu}{2\pi}\left(b_2^2 + \frac{(b^e)^2}{1-\nu} \right) \ln\left(\frac{l}{\rho}\right) + C^{dd} + \Gamma^{dd}, \quad (4a)
$$

$$
\frac{E^{dp}}{L}(l) = -\frac{f_1 b_3(1-2\nu)}{2\pi(1-\nu)} \ln\left(\frac{l}{\rho}\right) + C^{dp} + \Gamma^{dp}, \quad (4b)
$$

$$
\frac{E^{pp}}{L}(l) = -\frac{f_1^2(3-4\nu)}{8\pi\mu(1-\nu)} \ln\left(\frac{l}{\rho}\right) + C^{pp} + \Gamma^{pp}, \quad (4c)
$$

where C^{dd}, C^{dp} and C^{pp} are elastic terms that are not dependent on l and the Γ terms are the core energy terms associated with each interaction.

Combining the three elastic interaction terms together with the difference in grain boundary energy between the two phases, the nucleation energy is expressed as

$$
\frac{E^{2D}}{L} = \Delta\gamma^{\alpha\beta}l + \frac{1}{8\pi(1-\nu)}\left(4\mu\left[(1-\nu)b_2^2 + (b^e)^2\right] \right.
$$
$$
\left. - \frac{f_1^2(3-4\nu)}{\mu} - 4f_1 b_3(1-2\nu) \right) \ln\left(\frac{l}{\rho}\right) \quad (5)
$$
$$
+ 2\Gamma^{\alpha\beta} + C,
$$

with C being the elastic terms not dependent on l.

Equation (5) predicts that when the elastic interactions are included, the quasi-2D nucleation energy is no longer

a decreasing function of l for a negative $\Delta\gamma^{\alpha\beta}$, but it increases first for small nuclei resulting in a nucleation barrier. This nucleation barrier allows GBs to remain in a metastable state even in quasi-2D systems like thin films. The critical length of the α nucleus is determined by solving $\frac{dE^{2D}(l)}{dl} = 0$ for l, which gives an analytical solution:

$$l^c = \frac{4\left[(1-\nu)b_2^2 + (b^e)^2\right]\mu^2 - 4\mu f_1 b_3 (1-2\nu) - f_1^2(3-4\nu)}{8\pi\mu\Delta\gamma^{\alpha\beta}(\nu-1)}.$$

(6)

The analysis presented so far shows that in both 3D and quasi-2D cases, the elastic interaction energy due to GB phase junctions can increase the GB transformation barrier. These nucleation barriers stabilize metastable GB structures from transforming to their ground states. They can also prohibit sampling of other GB states with the same or higher energy by fluctuations at finite temperature. The energy of the elastic interactions can have a significant influence on the transformation behavior away from GB critical points and near the equilibrium coexistence where $\Delta\gamma^{\alpha\beta}$ is small. To test the predictions of our theory we performed MD simulations of GB phase transformations. Using the derived theory we extract the GB phase junction core energy from the MD data, calculate the elastic energy contribution to the nucleation barrier, the critical nucleus size and make a direct comparison with the MD results.

As an example we have selected the $\Sigma29(520)[001]$ symmetric tilt grain boundary in tungsten (W) modeled with the EAM potential developed by Zhou *et al.* [47]. W was chosen because it is elastically isotropic, so its elastic energy should be described well by the developed theory. The shear modulus and Poisson ratio were found to be $\mu = 160.0$ GPa and $\nu = 0.280$ respectively. Previously, grand-canonical GB structure searches demonstrated multiple GB phases in several different W GBs [48, 49]. We selected this particular boundary because the GB structure search identified two distinct GB structures that correspond to two different grain translations, but are composed of the same number of atoms [50–52]. The latter property is convenient for our analysis because it allows us to create nuclei of a new GB phase at 0 K to calculate their energy and study GB phase transformations on the short MD times scale.

The α phase is the ground state with the 0 K energy $\gamma^{\alpha} = 2.342$ J/m^2 and the β phase is metastable with energy $\gamma^{\beta} = 2.418$ J/m^2. To study the finite-temperature stability of both GB structures we performed MD simulations of each boundary using the NVT ensemble at temperatures of 1500K, 2000K and 2500K. Initially we used relatively large GB areas with dimensions of $30\sqrt{29}a_0 \times 10a_0$.

The structures of the two grain boundary phases are shown in Fig. 2. In these simulations both GB structures remained stable and did not transform even after 120 ns of simulation at the highest temperature of 2500K. This already suggests that the transformation barriers are significant compared to the driving forces for nucleation and growth, such as those associated with GB free energy difference or the thermal fluctuations.
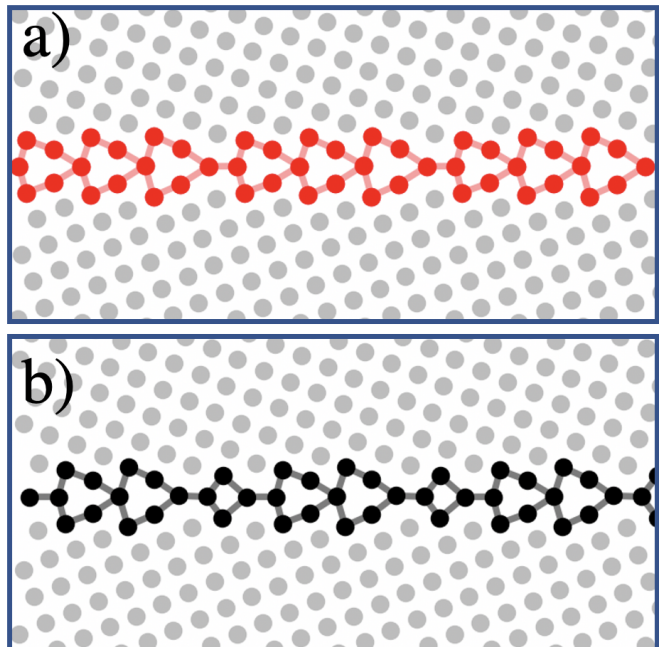

FIG. 2. Atomic structure of the two grain boundary phases. Panel a shows the α phase (ground state) and panel b shows the β phase (metastable).

To observe the GB phase transformations in MD we reduced the $\hat{e}_2$ dimension of the simulation block to the smallest possible value equal to just one lattice parameter making it quasi-2D. In this case the nucleation barrier is reduced significantly and after only 8 ns of MD simulation at 1500K the β phase transformed into the α phase by nucleation and growth. The same behavior was observed at higher temperatures, confirming that the β phase is metastable within the entire temperature range. These simulations clearly demonstrate that the GB structure observed in MD and GB phase transformation behavior is very sensitive to the choice of GB area, because for small dimensions periodic boundary conditions artificially influence the nucleation barrier. We used the simulation block containing both phases to calculate the Burgers vector of the GB phase junction following the methodology described in Ref. [42]. The Burgers vector was found to be $\boldsymbol{b} = 0.600\text{Å}\hat{\boldsymbol{e}}_1 + 0.423\text{Å}\hat{\boldsymbol{e}}_3$, which has the same order of magnitude as a disconnection for this grain boundary: $\boldsymbol{b}^{DSC} = -0.416\text{Å}\hat{\boldsymbol{e}}_1 - 0.416\text{Å}\hat{\boldsymbol{e}}_3$ [53, 54]. The tangential component of $\boldsymbol{b}$ is due to the different grain translations (or excess GB shears[55]) of the two GB phases and the normal component is equal to the difference in GB excess volumes [42–44]. The details of the Burger circuit analysis are included in the Supplemental Materials.

TABLE I. The relevant grain boundary properties for the two W GB phases. The other material properties are $\mu = 160.0$ GPa, $\nu = 0.280$ and $\Gamma^{\alpha\beta} = 0.383$ - 1.73 eV/Å.

grain boundary	γ (J/m^2)	τ_{11} (J/m^2)	τ_{22} (J/m^2)
α	2.342	3.926	3.609
β	2.418	0.138	5.775

To explain the surprising stability of the metastable GB phase β observed in the full 3D MD simulations, we could use our theory and predict the nucleation barriers. This would require calculations of finite-temperature elastic constants and free energies of all the defects involved including the free energy of GB junction cores. Some of those calculations are nontrivial and are beyond the scope of this study. However, we can still get valuable insights into the energetics of the GB phase transformation and validate our nucleation model by performing molecular statics calculations at 0 K. Knowing the Burgers vector of the GB phase junction from the MD analysis, GB energies, GB stresses and the material's elastic constants allows us to predict the nucleus energy as a function of its size. The last missing ingredient of the nucleation theory is the core energy of the GB phase junction $\Gamma^{\alpha\beta}$. To obtain $\Gamma^{\alpha\beta}$ we start our molecular statics analysis from the quasi-2D geometry. The simulation block with the GB had dimensions $120\sqrt{29}a_0 \times a_0 \times 10\sqrt{29}a_0$. With the small dimension along the GB tilt axis as before. By applying the appropriate initial translations to the upper and lower grains followed by an energy minimization we prepared bicrystals with the parent phase β containing a nucleus of phase α of different sizes. The method for constructing the grain boundary nucleus of size l is described in the Supplemental Materials. The nucleation energy is then calculated as the difference between total energies of the system with and without the nucleus.

Figure 3a shows an excellent agreement between the nucleation energy calculated directly from molecular statics (discrete blue points) and the predictions of the nucleation model (solid line) developed in this work. The critical nucleus for $\Sigma29(520)[001]$ from the molecular statics simulations was found to be l^{MD}=17.0 Å. $l^c = 21.6$ Å is predicted from Eq. (6). More importantly, Eq. (5) and the MD data predict $\Gamma^{\alpha\beta}_{min} = 0.383$ eV/Å for this geometry when the GB phase junction is parallel to the tilt axis. Similar to regular dislocations, the core energy $\Gamma^{\alpha\beta}$ may strongly depend on the line direction. By performing several quasi-2d calculations changing the GB phase junction direction, we found that $\Gamma^{\alpha\beta}_{min} = 0.383$ eV/Å and $\Gamma^{\alpha\beta}_{max} = 1.73$ eV/Å, where $\Gamma^{\alpha\beta}_{min}$ corresponds to $\boldsymbol{\xi} = [001]$ and $\Gamma^{\alpha\beta}_{max}$ corresponds to $\boldsymbol{\xi} = [\bar{2}50]$. To the best of our knowledge, these are the first reported values of GB phase junction core energy, and its directional anisotropy.
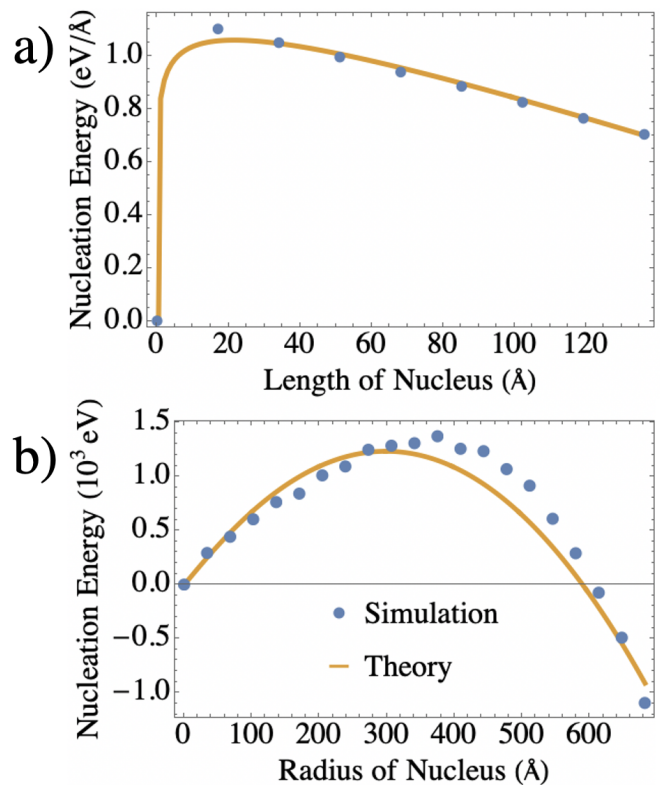

FIG. 3. Energy of the GB phase, α, nucleus created inside metastable GB phase, β, as a function of its size for a) quasi-2D and b) fully-3D geometries at 0K. The blue points correspond to the direct calculations using molecular statics, while the nucleation energy predicted by the model developed in this work is shown as a solid line.

Next, we tested the accuracy of the 3D model, by comparing its predictions to results of molecular statics simulations of circular nuclei. The computational details of these simulations are given in the Supplemental Materials. In this case, the GB had a roughly square shape with the block dimensions. The system contained 8.7 million atoms. The results of the analysis are shown in Fig. 3b. The nucleation energy predicted by Eq. (1) compares extremely well with the simulation results. For instance, the critical radius of the nucleus is predicted to be $R^c = 299$ Å, from the MD data the critical nucleus is found to have a radius of approximately 375 Å. The large nucleation barrier and critical nucleus size are consistent with the observation that GB transformation did not occur in our fully 3D simulations even at higher temperatures.

The critical nucleus sizes of the quasi-2D and fully 3D cases are vastly different with $l^c = 21.6$ Å (2D) compared to the critical diameter $D^c = 598$ Å(3D). This difference is not surprising because the contributions to the nucleation barrier scale differently with the nucleus size for these two geometries. However, this stark difference in critical radius points to the importance of simulat-

ing fully three dimensional systems for grain boundary phase nucleation. The consequences are borne out by MD simulation. In a thinner quasi-2D system, the transformation behavior depends strongly on the GB phase junction length. The α phase will nucleate at 1500 K after 8 ns with a repeat length of a_0 along $\hat{e}_2$, but no nucleation is seen even after 120 ns, when the repeat length is increased to $2a_0$.
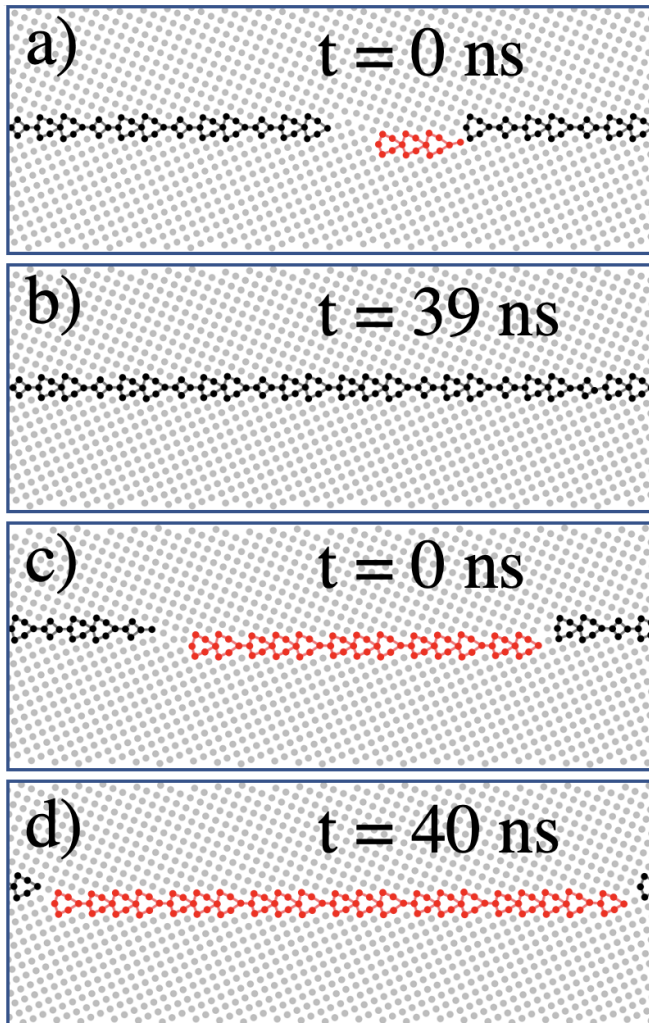

FIG. 4. The evolution of a dual-phase grain boundary system in MD simulation at T=1500K in a quasi-2D geometry. Panels a and b depict the shrinkage and ultimate annihilation of a subcritical length nucleus. Panels c and d depict the growth of a supercritical length nucleus. These simulations confirm the presence of nucleation barrier due to elastic interactions.

To further show that predictions of our nucleation model are not merely applicable to 0 K, we also performed high-temperature MD simulations. Specifically, using the quasi-2D geometry we prepared a dual phase system with a nucleus of the lowest free energy phase α embedded inside the metastable phase β. In one system the length of the α phase was less than the critical nu-

cleation length and in the other it was greater than the critical length estimated at 0 K; cf. Figure 4a and 4b, respectively. We then allowed the systems to evolve at 1500 K. As shown from Fig. 4a, the α nucleus of subcritical length shrinks and ultimately disappears from the simulation over the course of 40 ns. On the other hand, the nucleus of supercritical size grew, transforming the metastable boundary into its ground state α, as shown in Fig. 4b. These simulations confirm the presence of a nucleation barrier due to elastic interactions and show that the GB phase β can remain metastable even in a quasi-2D geometry.

Here we have derived a theory that describes homogeneous nucleation of GB phases. Our analysis recognizes that any GB phase junction necessarily contains a dislocation and a line force resulting from an imbalance in GB stresses. The theory quantifies the contributions from the elastic interactions and the core energy of the GB phase junction to the nucleation barrier. The predictions of the theory are in excellent agreement with the direct MD calculations. We find that the nucleation barriers are significant with the elastic interaction energy contributing about 25%, with the rest of the energy coming from the core energy of the junction.

Our finite-temperature MD simulations have shown that both GB phases studied remain stable and do not transform even at elevated temperatures, which is consistent with the large transformation barriers calculated at 0K. Our theory explains why away from critical points GBs cannot spontaneously change their structure even to a lower energy state. By quantifying the nucleation barrier one can in principle use the model to predict limits of metastability of different GB structures. While the analysis developed here has been applied to one particular boundary in tungsten, previous studies of GB phase transformations reported long nucleation times, sharp GB phase junctions and well defined nuclei [11, 20, 23, 38, 39, 48, 49], which suggests that the conclusions of this study are general.

Beyond first-order GB transformations discussed in this work, the analysis helps us better understand finite-temperature behavior of GBs in general. Prior studies suggested that at finite-temperature GBs sample higher energy states with Boltzmann probability, so that the GB structure is not unique but rather is represented by a properly weighted ensemble of different structures [27, 37]. Our study shows that the energy difference in the Boltzmann factor should also include the energy of the GB phase junction, in addition to the energy difference per unit area. At lower temperatures this positive energy can suppress phase fluctuations, resulting in the unique GB structure often observed in experiments.

By recognizing and quantifying the elastic energy of GB phase junctions, our study creates a foundation upon which further heterogeneous nucleation models can be developed.

ACKNOWLEDGEMENTS

—————

* winter24@llnl.gov
† frolov2@llnl.gov

[1] V. I. Kalikmanov, in *Nucleation Theory* (Springer, 2013) pp. 17–41.
[2] A. G. Khachaturyan, *Theory of Structural Transformations in Solids* (Dover Publications, Mineola, New York, 2008).
[3] D. A. Porter and K. E. Easterling, *Phase Transformations in Metals and Alloys* (CRC press, Cheltenham, United Kingdom, 1992).
[4] J. D. Eshelby, Proceedings of the Royal Society of London. Series A. Mathematical and Physical Sciences **241**, 376 (1957).
[5] J. D. Eshelby, Proceedings of the Royal Society of London. Series A. Mathematical and Physical Sciences **252**, 561 (1959).
[6] J. W. Cahn, Acta Metallurgica **5**, 169 (1957).
[7] P. R. Cantwell, M. Tang, S. J. Dillon, J. Luo, G. S. Rohrer, and M. P. Harmer, Acta Materialia **62**, 1 (2014).
[8] A. R. Krause, P. R. Cantwell, C. J. Marvel, C. Compson, J. M. Rickman, and M. P. Harmer, Journal of the American Ceramic Society **102**, 778 (2019).
[9] P. R. Cantwell, T. Frolov, T. J. Rupert, A. R. Krause, C. J. Marvel, G. S. Rohrer, J. M. Rickman, and M. P. Harmer, Annual Review of Materials Research **50**, 465 (2020).
[10] J. W. Gibbs, *The collected works of J. Willard Gibbs.*, Tech. Rep. (Yale Univ. Press,, 1948).
[11] K. L. Merkle and D. J. Smith, Phys. Rev. Lett. **59**, 2887 (1987).
[12] S. R. Phillpot and J. M. Rickman, The Journal of Chemical Physics **97**, 2651 (1992).
[13] E. Rabkin, C. Minkwitz, C. Herzig, and L. Klinger, Philosophical Magazine Letters **79**, 409 (1999).
[14] M. Tang, W. C. Carter, and R. M. Cannon, Phys. Rev. B **73**, 024102 (2006).
[15] S. von Alfthan, P. D. Haynes, K. Kaski, and A. P. Sutton, Phys. Rev. Lett. **96**, 055505 (2006).
[16] S. J. Dillon, M. Tang, W. C. Carter, and M. P. Harmer, Acta Materialia **55**, 6208 (2007).
[17] M. P. Harmer, Science **332**, 182 (2011).
[18] D. L. Olmsted, D. Buta, A. Adland, S. M. Foiles, M. Asta, and A. Karma, Phys. Rev. Lett. **106**, 046101 (2011).
[19] S. V. Divinski, H. Edelhoff, and S. Prokofjev, Phys. Rev. B **85**, 144104 (2012).
[20] T. Frolov, D. L. Olmsted, M. Asta, and Y. Mishin, Nature Communications **4**, 1899 (2013).
[21] J. Rickman, H. Chan, M. Harmer, and J. Luo, Surface Science **618**, 88 (2013).
[22] T. Frolov, M. Asta, and Y. Mishin, Phys. Rev. B **92**, 020103 (2015).
[23] T. Meiners, T. Frolov, R. E. Rudd, G. Dehm, and C. H. Liebscher, Nature **579**, 375 (2020).
[24] J. Wei, B. Feng, R. Ishikawa, T. Yokoi, K. Matsunaga, N. Shibata, and Y. Ikuhara, Nature Materials **20**, 951 (2021).
[25] Y. Mishin, Nature materials **20**, 911 (2021).
[26] T. Frolov, S. V. Divinski, M. Asta, and Y. Mishin, Phys. Rev. Lett. **110**, 255502 (2013).
[27] R. G. Hoagland and R. J. Kurtz, Philosophical Magazine A **82**, 1073 (2002).
[28] J. Luo, H. Cheng, K. M. Asl, C. J. Kiely, and M. P. Harmer, Science **333**, 1730 (2011).
[29] T. Hu, S. Yang, N. Zhou, Y. Zhang, and J. Luo, Nature Communications **9**, 2764 (2018).
[30] S. J. Dillon, K. Tai, and S. Chen, Current Opinion in Solid State and Materials Science **20**, 324 (2016), grain boundary complexions -current status and future directions.
[31] J. Luo, H. Wang, and Y.-M. Chiang, Journal of the American Ceramic Society **82**, 916 (1999).
[32] S. A. Bojarski, S. Ma, W. Lenthe, M. P. Harmer, and G. S. Rohrer, Metallurgical and Materials Transactions A **43**, 3532 (2012).
[33] W. E. Frazier, G. S. Rohrer, and A. D. Rollett, Acta Materialia **96**, 390 (2015).
[34] G. S. Rohrer, Current Opinion in Solid State and Materials Science **20**, 231 (2016), grain boundary complexions -current status and future directions.
[35] T. J. Rupert, Current Opinion in Solid State and Materials Science **20**, 257 (2016).
[36] A. Khalajhedayati, Z. Pan, and T. J. Rupert, Nature Communications **7**, 10802 (2016).
[37] J. Han, V. Vitek, and D. J. Srolovitz, Acta Materialia **104**, 259 (2016).
[38] T. Frolov and Y. Mishin, The Journal of Chemical Physics **143**, 044706 (2015).
[39] C. O'Brien, C. Barr, P. Price, K. Hattar, and S. Foiles, Journal of Materials Science **53**, 2911 (2018).
[40] P. R. Cantwell, S. Ma, S. A. Bojarski, G. S. Rohrer, and M. P. Harmer, Acta Materialia **106**, 78 (2016).
[41] O. Schumacher, C. J. Marvel, M. N. Kelly, P. R. Cantwell, R. P. Vinci, J. M. Rickman, G. S. Rohrer, and M. P. Harmer, Current Opinion in Solid State and Materials Science **20**, 316 (2016).
[42] T. Frolov, D. L. Medlin, and M. Asta, Phys. Rev. B **103**, 184108 (2021).
[43] R. C. Pond and V. Vítek, Proceedings of the Royal Society of London. A. Mathematical and Physical Sciences **357**, 453 (1977).
[44] R. C. Pond, Proceedings of the Royal Society of London. A. Mathematical and Physical Sciences **357**, 471 (1977).
[45] J. Hirth and R. Pond, Acta Materialia **44**, 4749 (1996).
[46] J. Hirth, R. Pond, R. Hoagland, X.-Y. Liu, and J. Wang, Progress in Materials Science **58**, 749 (2013).
[47] X. Zhou, H. Wadley, R. Johnson, D. Larson, N. Tabat, A. Cerezo, A. Petford-Long, G. Smith, P. Clifton, R. Martens, and T. Kelly, Acta Materialia **49**, 4005 (2001).
[48] T. Frolov, Q. Zhu, T. Oppelstrup, J. Marian, and R. E. Rudd, Acta Materialia **159**, 123 (2018).
[49] T. Frolov, W. Setyawan, R. Kurtz, J. Marian, A. R. Oganov, R. E. Rudd, and Q. Zhu, Nanoscale **10**, 8253

(2018).

[50] G. Bishop and B. Chalmers, Scripta Metallurgica **2**, 133 (1968).

[51] A. P. Sutton, V. Vitek, and J. W. Christian, Philosophical Transactions of the Royal Society of London. Series A, Mathematical and Physical Sciences **309**, 1 (1983).

[52] A. P. Sutton, V. Vitek, and J. W. Christian, Philosophical Transactions of the Royal Society of London. Series

A, Mathematical and Physical Sciences **309**, 37 (1983).

[53] H. Grimmer, Scripta Metallurgica **8**, 1221 (1974).

[54] J. Han, S. L. Thomas, and D. J. Srolovitz, Progress in Materials Science **98**, 386 (2018).

[55] T. Frolov and Y. Mishin, Phys. Rev. B **85**, 224106 (2012).